

On the 5f electronic ground state in UGe_2 at ambient pressure

This article has been downloaded from IOPscience. Please scroll down to see the full text article.

2005 J. Phys.: Condens. Matter 17 2443

(<http://iopscience.iop.org/0953-8984/17/15/015>)

View [the table of contents for this issue](#), or go to the [journal homepage](#) for more

Download details:

IP Address: 129.252.86.83

The article was downloaded on 27/05/2010 at 20:38

Please note that [terms and conditions apply](#).

On the 5f electronic ground state in UGe₂ at ambient pressure

A N Yaresko^{1,6}, P Dalmas de Réotier², A Yaouanc², N Kernavanois^{2,3},
J-P Sanchez², A A Menovsky⁴ and V N Antonov⁵

¹ Max Planck Institute for Physics of Complex Systems, Dresden D-01187, Germany

² Commissariat à l'Energie Atomique, Département de Recherche Fondamentale sur la Matière Condensée, F-38054 Grenoble Cedex 9, France

³ Institut Laue-Langevin, BP 156, F-38042 Grenoble Cedex 9, France

⁴ Van der Waals-Zeeman Instituut, Universiteit van Amsterdam, 1018 XE Amsterdam, The Netherlands

⁵ Institute of Metal Physics, Vernadsky Street, 03142 Kiev, Ukraine

Received 16 December 2004, in final form 8 March 2005

Published 1 April 2005

Online at stacks.iop.org/JPhysCM/17/2443

Abstract

We report x-ray absorption and magnetic circular dichroism measurements performed at the M_{4,5} edges of uranium in the ferromagnetic superconductor UGe₂. The spectra are described with the LSDA + *U* electronic structure computation method. Combined with the analysis of the published (i) x-ray photoemission spectrum, (ii) electron–positron momentum density, and (iii) angular dependence of the de Haas–van Alphen frequencies, we infer for the Coulomb repulsion energy within the 5f electron shell $U \lesssim 2$ eV. This leads to $U/W \simeq 2$ where W is the bandwidth.

(Some figures in this article are in colour only in the electronic version)

1. Introduction

The discovery of superconductivity in the ferromagnet UGe₂ at high pressure [1] is attracting much attention. It is believed that the 5f electrons of uranium are itinerant and form Cooper's pairs at low temperature. This picture seems to be supported by the results of de Haas–van Alphen (dHvA) measurements [2–5]. However, it has been claimed that dHvA does not provide reliable information on the relative strength of the electronic correlations in the 5f shell [6], hence the interest in considering additional techniques to probe these correlations.

We first report x-ray magnetic circular dichroism (XMCD) measurements performed at the M_{4,5} edges of uranium which probe the magnetic character of the empty 5f density of states. The experimental spectra are compared to spectra calculated with the so-called LSDA + *U* method in which the local spin-density approximation (LSDA) is used and the strong 5f Coulomb

⁶ Permanent address: Institute of Metal Physics, Vernadsky Street, 03142 Kiev, Ukraine.

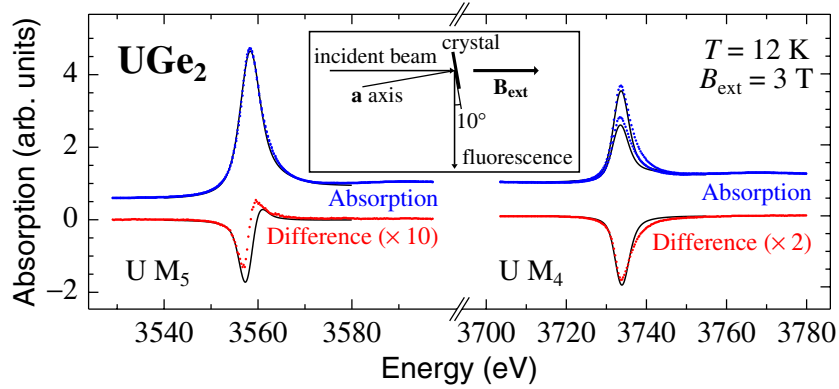


Figure 1. The dots show the measured uranium $M_{4,5}$ absorption and dichroism spectra of the ferromagnet UGe_2 (Curie temperature $T_C \simeq 52$ K and saturation magnetic moment of 1.42 (2) μ_B per formula unit, both values measured on our sample and consistent with the literature [9]). The data were obtained at 12 K and in an external field $B_{\text{ext}} = 3$ T. The experimental geometry is schematized in the inset. The \mathbf{a} axis is the easy axis. For each edge, two absorption spectra are presented, corresponding to the two opposite directions of the helicity of the incident x-ray beam. The solid lines result from the LSDA + U method with a screened Coulomb energy $U = 2$ eV. The intrinsic and experimental broadening mechanisms were accounted for by folding calculated XMCD spectra with Lorentzians of half-width of 2.2 and 3.2 eV and Gaussians of half-width of 1.6 and 1.5 eV for the M_4 and M_5 spectra, respectively. To compare the amplitudes of calculated and experimental XMCD spectra, we have normalized the calculated M_5 isotropic absorption spectrum to the measured one taking into account the background intensity. Then, the thus obtained normalization factor was used for the M_4 absorption and $M_{4,5}$ XMCD spectra.

repulsion U is described by a Hubbard-like model treated at the Hartree–Fock level. The value found for U is compatible with the one obtained by Shick and Pickett who were able to reproduce the total moment and the magnetocrystalline anisotropy of UGe_2 [7]. To further test the model the inferred $5f$ density of states is used to discuss data obtained by other microscopic techniques: x-ray (XPS) and ultraviolet (UPS) photoemission spectroscopies, bremsstrahlung isochromat spectroscopy (BIS) and electron–positron momentum density (EPMD) and dHvA measurements. A combined analysis of all the results provides an estimate for U larger than previously inferred.

2. X-ray absorption: measurements and sum rule analysis

The XMCD measurements were carried out at the ESRF beamline ID12A. A description of the experimental method as applied to uranium is given elsewhere [8]. The spectra were recorded in the fluorescence-yield detection method. They have been corrected for self-absorption to give the absorption spectra, using a well established procedure. The results are shown in figure 1.

A well defined two-lobe structure, a low-energy negative lobe and a high-energy positive lobe, is found at the M_5 edge. Such a structure has already been detected for UPd_2Al_3 , UBe_{13} , UPt_3 , $U_{0.3}La_{0.7}S$ and $U_{0.4}La_{0.6}S$ [10, 11] and $UPtAl$ [12]. On the other hand, the XMCD spectrum at the M_5 consists mainly of one lobe for US , $U_{0.6}La_{0.4}S$, $USb_{0.5}Te_{0.5}$, UFe_2 , URu_2Si_2 , $URhAl$ [10, 11] and $UCoAl$ [12]. The appearance of two lobes is a finger-print of (i) an appreciable density of empty $j = 7/2$ sublevels with both negative and positive $m_{7/2}$ and (ii) a sufficient energy spread over these sublevels [13, 10]. We have used here the jj -coupling scheme where the total momentum \mathbf{j} is written as $\mathbf{j} = \mathbf{l} + \mathbf{s}$. However, the combination of the

hybridization, Coulomb, exchange and crystal-field energies may be so large relative to the 5f spin-orbit energy that the jj -coupling is no longer a good approximation. A toy model provides a vivid demonstration [14].

Quantitatively we first focus on values of moments of the 5f shell at saturation. The orbital magnetic moment can be estimated from the first XMCD sum rule [15, 16]. We get $\mu_L = 1.91$ (19) and 1.75 (17) μ_B for the hypothetical f^2 and f^3 configurations, respectively. The analysis of the magnetic form factor also provides an estimate for μ_L . Kernavanois *et al* [17] find $\mu_L = 2.37$ (4) and 2.62 (4) μ_B for the f^2 and f^3 configurations respectively and Kuwahara *et al* [18] give $\mu_L = 2.20$ (3) and 2.43 (3) μ_B , respectively. Although the dispersion of the values is rather large, μ_L is definitively smaller than $3 \mu_B$. We shall refer to this bound value when comparing experimental and LSDA + U results. The total magnetic moment of the 5f electrons, μ , is also determined by neutron diffraction. It is found to be almost equal to the bulk magnetization at saturation. Then the ratio $R = -\mu_L/\mu_S$ of the orbital to spin moment can be computed. One set of measurements gives $R = 2.60$ (15) and 2.24 (10) for the f^2 and f^3 configurations, respectively [17]. The other set leads to values $\sim 10\%$ higher [18]. The second XMCD sum rule allows us to estimate $2\langle S_z^e \rangle / (3n_h)$ [19, 16]. n_h is the number of holes in the 5f shell and $\langle S_z^e \rangle$ the expectation value of an effective spin operator defined as $S_z^e = S_z + 3T_z$. T_z and S_z are the z projections of the magnetic dipole and spin operators, respectively. We have $2\langle S_z^e \rangle / (3n_h) = 0.075$ (13).

Another sum rule expresses the expectation value for the spin-orbit operator of the valence states in terms of the branching ratio of the core-valence transitions [16]. Its validity for actinides has been checked recently [20]. In the case of the $M_{4,5}$ edges, this sum rule is written $\langle w^{110} \rangle / n_h = -(5/2)(B - 3/5) + \Delta$ where $\langle w^{110} \rangle$ is the expectation value for the angular part of the 5f spin-orbit electron operator, B the branching ratio ($B \equiv A_{5/2} / (A_{5/2} + A_{3/2})$ where $A_{5/2}$ and $A_{3/2}$ are the areas underneath the M_5 and M_4 edges excluding the background) and Δ a small correction term ($\Delta = -0.018$). Since we measure $B = 0.66$, we estimate $\langle w^{110} \rangle / n_h = -0.17$. Thus this suggests an f^2 electronic structure [20]. However, the determination of $\langle w^{110} \rangle / n_h$ requires a very precise value for B since its numerical value is not far from the number $3/5$ which is subtracted from it. For example, if we take $B = 0.68$, we compute $\langle w^{110} \rangle / n_h = -0.22$, suggesting a structure close to f^3 . The fluorescence-yield detection method we use is not capable of such precision because of the corrections it implies. The problem of precision is not so stringent for the other two sum rules used above.

3. X-ray absorption: LSDA + U analysis

The absorption spectra at the two edges are structureless. Therefore, multiplet effects are negligible [13]. This justifies the description of the absorption of the incident x-rays in terms of a one-particle approximation. Hence, valuable information on the nature of the 5f electrons can be obtained from comparison of experimental data to results of band-structure calculations. In the present work the electronic band structure and absorption and XMCD spectra have been calculated within LSDA using the spin-polarized relativistic linear muffin-tin orbital method [21]. The calculations have been performed for the crystal structure of [22]. The strong electronic correlations in the 5f shell have been taken into account by using the rotationally invariant LSDA + U method [23, 24]. The effective on-site Coulomb repulsion U was considered as an adjustable parameter and its value was refined by comparing calculated results to available experimental data. Calculations were performed for U varying from 0.5 to 4.0 eV with 0.5 eV increment. $U = 4$ eV is derived from constrained LSDA calculations. As such calculations tend to overestimate U in uranium compounds, 4 eV seems to be the upper limit for the effective Coulomb repulsion. For the exchange integral J the value of 0.5 eV

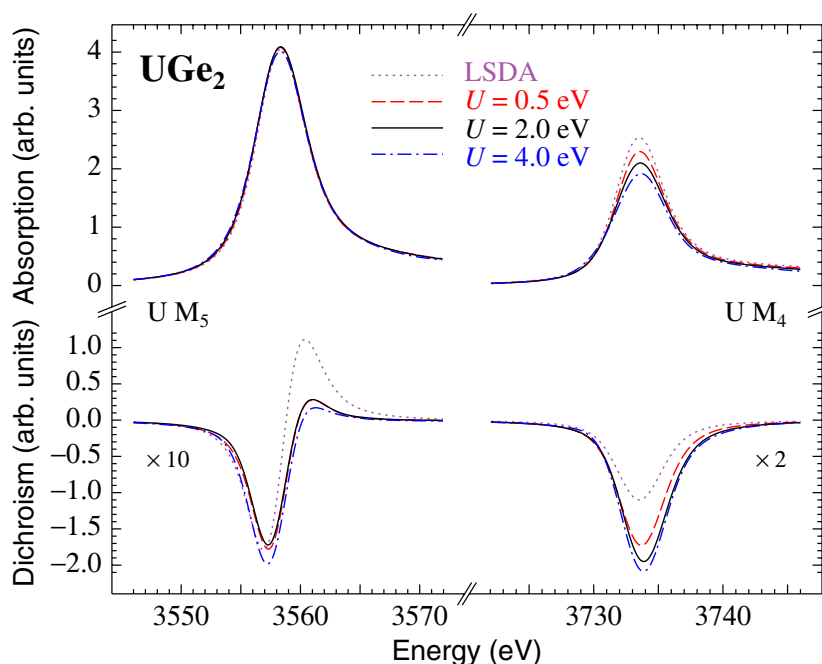


Figure 2. $M_{4,5}$ absorption and XMCD spectra computed for UGe_2 using the LSDA+ U method for different values of U . Information on the convolution and normalization of the spectra is given in the caption of figure 1. The M_5 XMCD spectra for $U = 0.5$ and 2 eV can hardly be distinguished in the plot.

estimated from constrained LSDA calculations was used. Further details of the calculations are given elsewhere [25].

The x-ray absorption and XMCD spectra are reasonably well described assuming U in the range 0.5–2 eV. Figure 1 shows the results with $U = 2$ eV since this value gives a more consistent interpretation of other data (see below). The main misfit occurs at the M_5 XMCD spectrum: although the two-lobe structure is reproduced, their amplitudes are not and the calculated spectrum is slightly too wide at high energy. In figure 2 we compare theoretical spectra for different values of U . All the calculations reproduce the two-lobe structure. The amplitude of the M_5 negative lobe is approximately independent of U . The amplitude of the positive lobe in the case $U = 0$ is strongly overestimated whereas the one of the M_4 spectrum is half that in the experiment. Thus, for UGe_2 , as for many other uranium compounds [25], the LSDA based calculations cannot reproduce the M_5 and M_4 XMCD spectra. While the spectra computed for $U = 2$ eV are close to the experimental ones, the disagreement is appreciable when $U = 4$ eV. This is in line with the fact that the XMCD spectrum at the M_5 edge is inconsistent with the atomic model for which the whole 5f density is localized [14]. We notice that the relative intensity of the M_4 absorption spectrum decreases as U increases and, thus, not only XMCD but also absorption spectra reflect electronic correlations effects.

To better understand the dependence of the theoretical spectra on the value of U , let us compare in more detail the results of the LSDA and LSDA+ U calculations. According to LSDA, the 5f charge is equal to 2.837, the 5f states are situated at the minimum of the density of Ge p states and their hybridization with the latter is relatively weak. $5f_{5/2}$ states give a dominant contribution of 1.993 to the total 5f charge. The maximum of the $5f_{7/2}$ density of

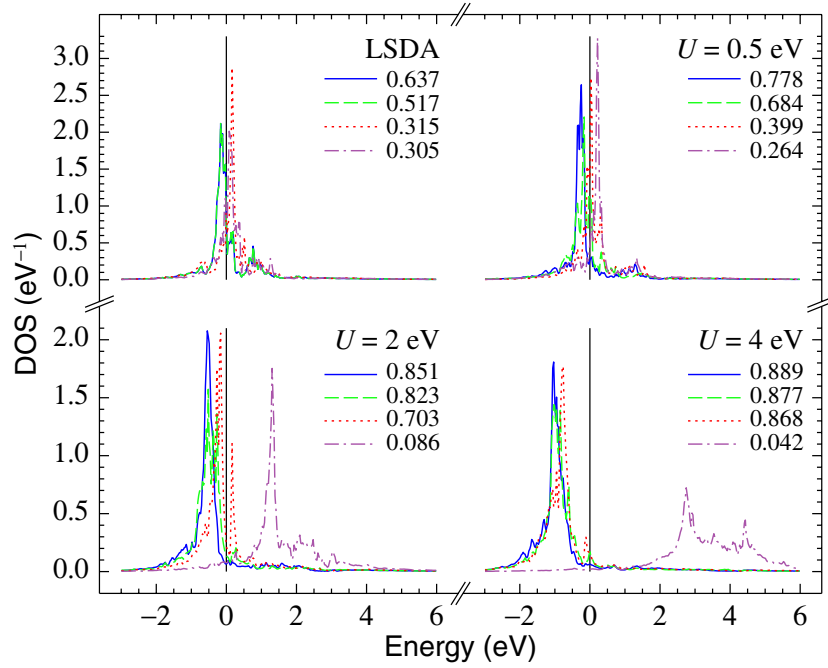


Figure 3. Orbital projected DOS for the four most populated orbitals for different values of U . The vertical full lines give the Fermi level relative to which the energy is measured. The occupation numbers for the different orbitals are indicated. For $U = 0$ eV (LSDA), two other orbitals (not shown) have non-negligible occupation numbers. Note that even at $U = 4$ eV the DOS at the Fermi energy does not vanish.

states (DOS) is found at ~ 1.5 eV above the Fermi level. However, these states contribute 0.844 electron to the net 5f charge. As U increases the 5f charge also increases but only slightly and even for $U = 4$ eV it is 2.964, i.e. less than the value of 3 expected for the U^{3+} ion. The balance between the $5f_{5/2}$ and $5f_{7/2}$ charges is more affected when U increases: the net $5f_{5/2}$ charge is 2.648 for $U = 4$ eV. As the average occupation of $5f_{7/2}$ states is rather small, they are pushed to higher energies by the Coulomb repulsion and their contribution to the net 5f charge decreases. Since the major contribution to the absorption at the M_4 edge stems from the $3d_{3/2} \rightarrow 5f_{5/2}$ transitions and that at the M_5 edge originates primarily from $3d_{5/2} \rightarrow 5f_{7/2}$ transitions [13], the decrease of the number of empty $5f_{5/2}$ states is responsible for the change of relative intensity of the M_4 absorption spectra.

A qualitative explanation to the XMCD spectra shape is provided by the analysis of the orbital character and occupation numbers of individual 5f orbitals. In the most general way these orbitals can be defined as the eigenvectors that diagonalize the 5f occupation matrix n_{m_l, m_s, m'_l, m'_s} where m_l and m_s are the azimuthal and spin quantum numbers, respectively. The corresponding eigenvalues can be interpreted as orbital occupation numbers.

In contrast to 5f charges, the orbital character and the occupation numbers of 5f orbitals are more sensitive to the value of U . Already when only the angular correlations in the 5f shell are accounted for in LSDA+ U calculations, that is when $U = J = 0.5$ eV, the difference in orbital occupancies increases as compared to LSDA calculations. The occupation of the three most populated orbitals increases, whereas orbitals with strong $m_{3/2}$ and $m_{5/2}$ character are pushed to higher energies by the Coulomb repulsion and become empty. Because of the increased

Table 1. Computed physical quantities for UGe₂ as a function of U : spin μ_S , orbital μ_L and total magnetic moment μ , ratios $R \equiv -\mu_L/\mu_S$ and $2\langle S_z^e \rangle / (3n_h)$, expectation value of the magnetic dipole term $\langle T_z \rangle$ and of the spin-orbit operator per hole $\langle w^{110} \rangle$ of the uranium 5f shell; spin moments of the three inequivalent Ge ions. $m\mu_B$ stands for $10^{-3}\mu_B$.

U eV	μ_S μ_B	μ_L μ_B	μ μ_B	R	$\frac{2\langle S_z^e \rangle}{(3n_h)}$	$\langle T_z \rangle$	$\frac{\langle w^{110} \rangle}{n_h}$	μ_{Ge_1} $m\mu_B$	μ_{Ge_2} $m\mu_B$	μ_{Ge_3} $m\mu_B$
0.0	-1.39	1.94	0.55	1.40	0.058	0.094	-0.162	-9	-10	8
0.5	-1.47	3.04	1.57	2.07	0.078	0.190	-0.213	-9	-18	11
2.0	-1.54	3.46	1.92	2.25	0.087	0.227	-0.259	-10	-27	14
3.0	-1.58	3.62	2.04	2.29	0.091	0.238	-0.278	-5	-23	14
4.0	-1.64	3.76	2.12	2.29	0.094	0.245	-0.291	-4	-17	0

asymmetry in occupations of the states with positive and negative m_j , the cancellation of the contributions of opposite signs to XMCD spectra originating from dipole allowed transitions with $\delta m_j = \pm 1$, i.e. those corresponding to absorption of photons with opposite helicities, becomes less effective and the intensity of the M_4 XMCD spectrum increases, as noticed in figure 2. The effect of the orbital polarization on the M_5 XMCD spectrum is more subtle. The relative occupation of orbitals formed by the $5f_{7/2}$ states does not change. However, because of the increased orbital polarization of $5f_{5/2}$ states, the LSDA + U potential acting on $5f_{7/2}$ orbitals becomes strongly dependent on their angular character. This leads to energy redistribution among the $5f_{7/2}$ states which causes the decrease of the magnitude of the positive lobe in the M_5 XMCD spectrum.

The difference in orbital occupation increases with U as seen in figure 3. For $U = 2$ eV the two most populated 5f orbitals become almost completely occupied and corresponding peaks of orbital resolved DOS are found below the Fermi energy, E_F . In spite of the increase of its occupation, the third most occupied orbital remains only partially occupied at $U = 2$ eV. Whereas the main peak of DOS projected onto this orbital is situated below E_F , an additional narrow peak can be seen just above the Fermi level. When U is increased to 4 eV the maxima of all three DOS curves shift to -1 eV below E_F and the occupancies become close to 0.9. However, orbital projected DOS has a peak just at the Fermi level even for this large value of U .

We now compare measured moments to theoretical predictions; see table 1. LSDA calculations underestimate μ while it is well reproduced by an LSDA + U with $U = 0.7$ eV and $J = 0.44$ eV [7]. Our LSDA + U calculation with $U = J = 0.5$ eV also gives a reasonable μ value. R and $2\langle S_z^e \rangle / (3n_h)$ are not in strong disagreement with experiment for U in the range 0.5–2 eV while μ_L and μ are clearly overestimated for $U \geq 0.5$ eV. This discrepancy of order 30% is usual with the LSDA + U method: being based on a Hartree-Fock approximation, it tends to overestimate the degree of the symmetry breaking [24]. Calculated Ge magnetic moments are collected in the last three columns of table 1. Notwithstanding the strong magnetization of the 5f shell, the Ge moments are very small and their modulus does not exceed $0.03 \mu_B$ which is in a good agreement with the neutron results [17].

For completeness, we provide in table 1 calculated values of $\langle T_z \rangle$ and $\langle w^{110} \rangle / n_h$ as a function of U . As expected $\langle T_z \rangle$ is not negligible. $\langle w^{110} \rangle / n_h$ is in the expected range. If measured, this latter physical quantity would give us a way to estimate U .

To summarize the absorption and XMCD spectrum interpretation, we have shown that the model in which all 5f states are treated within the LSDA approximation (i.e. $U = 0$) cannot reproduce the experimental data. A value of U in the range 0.5–2 eV is needed.

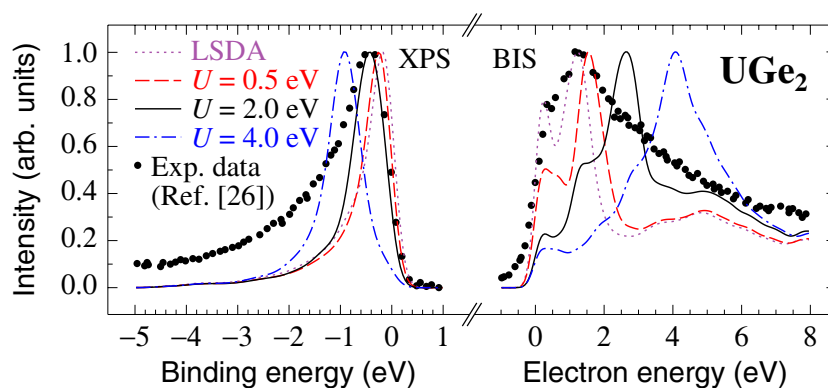


Figure 4. XPS and BIS spectra are compared to theoretical predictions. The experimental XPS spectrum has been obtained from the difference of spectra recorded at the $5d \rightarrow 5f$ resonance and off resonance i.e. with photons of respective energies 97 and 92 eV. It is compared with theoretical 5f partial DOS. The experimental BIS spectrum is compared to computed total DOS curves. The measured spectra are wider than predicted, reflecting at least partly the one-electron nature of the LSDA + U method [26]. The theoretical spectra have been convoluted with a Gaussian of half-width of 0.25 eV.

4. Analysis of other published data

To further test and refine these conclusions, we now analyse published data.

The energy position of the broad peak observed in the on–off resonance XPS data shown in figure 4 is best reproduced by the LSDA + U model with U in the range 1.5–2 eV. In order to achieve reasonable agreement in the position of the peak at ~ 0.2 eV in the UPS spectrum measured with photons of 40 eV (not shown in figure 4) the value of U should be reduced to 0.5–1.5 eV. However, since the escape depth for photoelectrons with these kinetic energies is very small the shift of the experimental peak towards the Fermi level can be caused by increased contribution of U ions in the surface layers [26]. The BIS spectrum (also shown in figure 4) clearly excludes $U \geq 3$ eV. Best predictions are obtained for $U \leq 0.5$ eV. However, these calculations strongly underestimate the intensity in the energy range between 2 and 5 eV. A possible reason for the discrepancy is that BIS spectra contain information that cannot be described by band theory, such as the two-electron bound state formed in the final state [26].

Recent measurements [27] indicate the presence of a sharp peak at the Fermi level (E_F) in the high-resolution UPS (He II α) spectrum of UGe₂. The peak was interpreted as the ‘coherent U 5f’ peak originating in the itinerant U 5f electrons, whereas a broad shoulder at ~ 0.5 eV binding energy was attributed to the ‘incoherent part’ representing localized 5f electrons. From the comparison of the calculated U 5f DOS to the experimental spectrum we can conclude that neither LSDA nor LSDA + U calculations can reproduce the intense peak at E_F . The LSDA calculation results in a rather high U 5f DOS peak at the Fermi level but its width is significantly larger than in the experiment. Moreover, the shoulder at higher binding energies is completely missing. The LSDA + U calculations with U between 1 and 2 eV do produce a peak of DOS which could be associated with the broad shoulder. However, it is much too high compared to the DOS peak just below E_F . The reason for this discrepancy between the theory and the experiment is still unclear.

The published EPMD is compared to projected electronic occupancies for different electronic configurations in figure 5. Only the map for $U = 2$ eV is in fairly good agreement

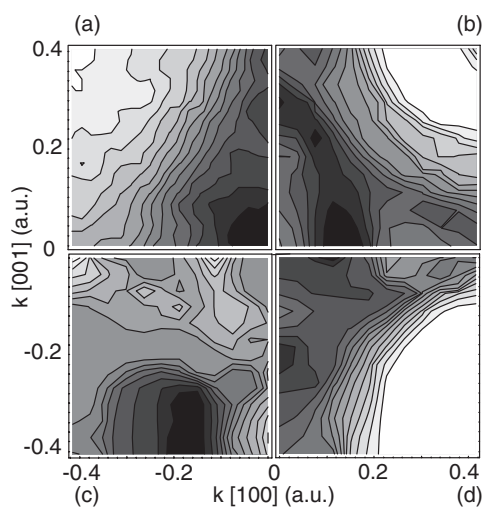


Figure 5. Experimental projected EPMD in the a^*c^* plane at 60 K for UGe_2 [6] in quadrant (a). The contour level spacing corresponds to 0.4% of the maximum. This density is compared to two-dimensional electronic occupancies computed with the LSDA + U method. Quadrants (b), (c), and (d) present respectively the results for $U = 4, 0.5$ and 2 eV. The theoretical maps are convoluted as explained in [6]. One Bloch vector in atomic units is equal to 1.89 \AA^{-1} . White colour corresponds to high occupancy and black to low occupancy.

with the shape of the experimental density. The map for $U = 4$ eV and the f^3 -core configuration [6] also have the proper symmetry. However, a local minimum is computed at the corner of the Brillouin zone, in contrast to the measured density.

A close look at the published values of the dHvA frequencies indicates a consistent set of data only for \mathbf{B}_{ext} parallel to the \mathbf{b} crystal axis for which frequencies of about 9000 T are observed [2–5]. Our calculations of the angular dependence of the dHvA frequencies reproduce reasonably well the experimental results for the high-frequency branch, except for the LSDA + U calculations with U in the range 0.5–1 eV and the f^2 -core configuration. However, the LSDA calculation produces a hole-like Fermi surface [28], in contradiction to the positron data [6]. The LSDA + U calculations with $U > 1$ eV and the LSDA one for the f^3 -core configuration yield positive effective masses, i.e. the corresponding sheet of the Fermi surface is electron-like, in agreement with the positron data. The masses are relatively light, between 2 and $7 m_0$, depending on the \mathbf{B}_{ext} orientation (m_0 is the bare electron mass). A detailed comparison between the theory and the experiment for low dHvA frequencies is, unfortunately, practically impossible because of a very large number of branches in the range 0.1–1 kT.

The disagreement between the dHvA results calculated for small values of U and the experiment sets the lower bound for the value of U to 1.5 eV. It should be pointed out, however, that, being based on a mean-field approximation, the LSDA + U can hardly provide a reliable description of the Fermi surface of strongly correlated metals.

5. Conclusions and outlook

In conclusion, an interpretation of absorption and XMCD $M_{4,5}$ spectra, XPS profile, two-dimensional EPMD and angular dependence of the frequencies of dHvA oscillations cannot be achieved with fully itinerant $5f$ states. The LSDA + U model with a Coulomb repulsion

energy within the 5f shell approximately equal to 2 eV is required. U is therefore larger than the commonly assumed value of ~ 0.5 eV [7]. Since the full width at half maximum of the 5f band is computed to be $W \simeq 0.8$ eV, $U/W \simeq 2$. For a more precise determination of U and W , in particular estimates of the uncertainty on the parameter values, a better theoretical model is needed. The dynamical mean-field theory recently introduced for actinides may address this issue [29]. In addition, more experimental data would be welcome to refine the value of U . It would also be interesting to test the applicability of the scenario in which some U 5f states are localized while others remain itinerant [30] to the case of UGe₂. Finally, we note that extremely small magnetic moments for the diffuse electrons have been observed [31, 17, 18]. To explain these data, a reliable computation of the dynamical susceptibility has to be carried out.

Acknowledgments

We gratefully acknowledge A Rogalev for the excellent working conditions at beamline ID12A of ESRF and M Biasini for providing the EPMD map. We are thankful to P Fulde for helpful discussions.

References

- [1] Saxena S S *et al* 2000 *Nature* **406** 587
- [2] Satoh K, Yun S W, Umehara I, Ōnuki Y, Uji S, Shimizu T and Aoki H 1992 *J. Phys. Soc. Japan* **61** 1827
- [3] Terashima T, Matsumoto T, Terakura C, Uji S, Kimura N, Endo M, Komatsubara T and Aoki H 2001 *Phys. Rev. Lett.* **87** 166401
- [4] Terashima T, Matsumoto T, Terakura C, Uji S, Kimura N, Endo M, Komatsubara T, Aoki H and Maezawa K 2002 *Phys. Rev. B* **65** 174501
- [5] Settai R, Nakashima M, Araki S, Haga Y, Kobayashi T C, Tateiwa N, Yamagami H and Ōnuki Y 2002 *J. Phys.: Condens. Matter* **14** L29
- [6] Biasini M and Troc R 2003 *Phys. Rev. B* **68** 245118
- [7] Shick A B and Pickett W E 2001 *Phys. Rev. Lett.* **86** 300
- [8] Dalmas de Réotier P *et al* 1997 *J. Phys.: Condens. Matter* **9** 3291
- [9] Ōnuki Y, Ukon I, Yun S W, Umehara I, Satoh K, Fukuhara T, Sato H, Takayanagi S, Shikama M and Ochiai A 1992 *J. Phys. Soc. Japan* **61** 293
- [10] Dalmas de Réotier P and Yaouanc A 2002 *Physica B* **318** 272
- [11] Yaouanc A, Dalmas de Réotier P and van der Laan G 2004 *Phys. Rev. Lett.* **93** 019701
- [12] Kučera M, Kuneš J, Kolomiets A, Diviš M, Andreev A V, Sechovský V, Kappler J P and Rogalev A 2002 *Phys. Rev. B* **66** 144405
- [13] Dalmas de Réotier P, Yaouanc A, van der Laan G, Kernavanois N, Sanchez J P, Smith J L, Hiess A, Huxley A and Rogalev A 1999 *Phys. Rev. B* **60** 10606
- [14] Yaouanc A, Dalmas de Réotier P, van der Laan G, Hiess A, Goulon J, Neumann C, Lejay P and Sato N 1998 *Phys. Rev. B* **58** 8793
- [15] Thole B T, Carra P, Sette F and van der Laan G 1992 *Phys. Rev. Lett.* **68** 1943
- [16] van de Laan G and Thole B T 1996 *Phys. Rev. B* **53** 14458
- [17] Kernavanois N, Grenier B, Huxley A, Ressouche E, Sanchez J P and Flouquet J 2001 *Phys. Rev. B* **64** 174509
- [18] Kuwahara K *et al* 2002 *Physica B* **312/313** 106
- [19] Carra P, Thole B T, Altarelli M and Wang X 1993 *Phys. Rev. Lett.* **70** 694
- [20] van der Laan G, Moore K T, Tobin J G, Chung B W, wall M A and Schwartz A J 2004 *Phys. Rev. Lett.* **93** 097401
- [21] Andersen O K 1975 *Phys. Rev. B* **12** 3060
- [22] Oikawa K, Kamiyama T, Asano H, Ōnuki Y and Kohgi M 1996 *J. Phys. Soc. Japan* **65** 3229
- [23] Liechtenstein A I, Anisimov V I and Zaanen J 1995 *Phys. Rev. B* **52** R5467
- [24] Yaresko A, Antonov V and Fulde P 2003 *Phys. Rev. B* **67** 155103
- [25] Antonov V, Harmon B and Yaresko A 2004 *Electronic Structure and Magneto-Optical Properties of Solids* (Dordrecht: Kluwer–Academic)
- [26] Suzuki S *et al* 1993 *Japan. J. Appl. Phys. Series* **8** 59

-
- [27] Ito T, Kumigashira H, Souma S, Takahashi T, Haga Y and Onuki Y 2002 *J. Phys. Soc. Japan* **71** (Suppl.) 261
- [28] Yaresko A and Thalmeier P 2004 *J. Magn. Magn. Mater.* **272–276** E391
- [29] Savrasov S Y, Kotliar G and Abrahams E 2001 *Nature* **410** 793
- [30] Zwicky G, Yaresko A and Fulde P 2002 *Phys. Rev. B* **65** 081103
- [31] Yaouanc A, Dalmas de Réotier P, Gubbens P C M, Kaiser C T, Menovsky A A, Mihalik M and Cottrell S P 2002 *Phys. Rev. Lett.* **89** 147001